Tumor-Derived Matrix Metalloproteinase-1 Targets Endothelial Proteinase-Activated Receptor 1 Promoting Endothelial Cell Activation

Tobias Goerge,[1,6] Alexej Barg,[2] Eva-Maria Schnaeker,[1] Birgit Poppelmann,[1] Victoria Shpacovitch,[1] Anke Rattenholl,[1] Christian Maaser,[5] Thomas A. Luger,[1,4] Martin Steinhoff,[1,3] and Stefan W. Schneider[1]

[1]Department of Dermatology, [2]Institute of Physiology II, [3]Interdisziplinäres Zentrum für Klinische Forschung Münster; [4]Ludwig Boltzmann Institute for Immunobiology and Cell Biology of the Skin; and [5]Department of Medicine B, University of Münster, Münster, Germany; and [6]Center for Blood Research Institute for Biomedical Research, Department of Pathology, Harvard Medical School, Boston

Abstract

In the vascular system, circulating tumor cells interact with endothelial cells. Tumor-endothelial cross-talk transforms the intravascular milieu to a prothrombotic, proinflammatory, and cell-adhesive state called endothelial cell activation (ECA). In the present study, we analyze the potential of metastatic tumor-derived soluble factors to transform the vascular endothelium into a prothrombotic and proinflammatory activated state. Supernatant from cultured melanoma and colon cancer cells (A375, WM9, A7, and HT-29) induced an acute activation of macrovascular and microvascular endothelial cells (human umbilical vein endothelial cells and human dermal microvascular endothelial cells) as shown by intracellular calcium flux and secretion of von Willebrand factor and interleukin-8, all markers of acute ECA. This process was inhibited using specific proteinase-activated receptor 1 (PAR1) inhibitors (RWJ-58259 and SCH-79797), indicating a mediating role for endothelial thrombin receptors. Immunofluorescence, Western blot analysis, and collagenase activity assay of tumor cells and culture supernatant revealed the presence of matrix metalloproteinase-1 (MMP-1), a recently described activator of PAR1. Inhibition of MMP-1 in supernatant from cultured tumor cells significantly attenuated ECA. Additional studies using isolated human MMP-1 (5 nmol/L) proved the presence of a functional MMP-1/PAR1 axis in tumor-endothelial communication. These findings show a new pathway of tumor-endothelial cross-talk via an intravascular MMP1/PAR1 axis in microvascular and macrovascular endothelium. Inhibition of this cross-talk may be a powerful means to prevent tumor-induced ECA and thus thrombotic and inflammatory cell adhesion. (Cancer Res 2006; 66(15): 7766-74)

Introduction

Proteinase-activated receptors (PAR) are a unique class of G-protein-coupled receptors that are characterized by a distinctive mechanism of activation. Proteolytic cleavage at the NH_2 terminus of the receptor reveals a tethered ligand that binds to the second extracellular loop on the same receptor and thus activates it intramolecularly. Thus far, the PAR family comprises four members defined as PAR1 to PAR4 (1). They have been shown to play an important role in various pathophysiologic settings, particularly in inflammatory and coagulatory vascular diseases, as shown by their abundant expression on platelets and endothelium (2, 3). In addition, PAR1, a well-investigated member of the PAR family formerly known as thrombin receptor, has been shown to play an important role in neoplastic disease. Previous studies have shown clearly a PAR1-mediated increase of invasivity and metastatic potential in different tumor entities *in vitro* and *in vivo*, including cancers of the breast, colon, prostate, and melanoma (4–7). In addition, available data indicate a correlation of PAR1 expression in tissue with the degree of tumor spreading (4, 8). The role of tumor-expressed PAR1 in tumorigenesis is further underlined by studies showing hematogenous metastases dependent on thrombin, the prototypical activator of PAR1. Nierodzik et al. (9) showed already in a mouse model that thrombin-enhanced experimental pulmonary metastases of melanoma are related to PAR1 expression (9). Moreover, thrombin treatment of tumor cells induces a metastatic phenotype (10, 11). These reports clearly suggest an invasive and tumorigenic potential of PAR1 activation expressed by cancer cells.

Apart from thrombin, several other proteases (FXa, trypsin, granzyme A, and APC) were shown to be capable of activating PAR1 (see refs. 2, 3 for review). However, for a long time, the activation of tumor-expressed PAR1 remained elusive. Only recently, Boire et al. (12) reported that matrix metalloproteinase (MMP)-1, a collagenase of the MMP family, is an additional proteolytic activator of PAR1 promoting invasion and tumorigenesis of breast cancer cells *in vitro* and *in vivo*. The discovery of a functional MMP-1/PAR1 interaction was inspired by the concept that host-derived MMP-1 cleaves tumor-expressed PAR1, thus promoting the metastatic potential of cancer cells (13).

The finding of PAR1 activation by MMP-1 allowed us to hypothesize that this interaction could also contribute to tumor-host communication in the vascular milieu. MMPs are abundantly secreted by tumor cells themselves, and we reported previously an important role of secreted MMPs in melanoma invasion (14, 15). Additionally, expression of PAR1 on vascular endothelium is well documented, and tumor-endothelial interactions represent a crucial step in tissue colonization by tumor cells moving through the vascular compartment (hematogenous metastasis). Therefore, we postulated that tumor-endothelial cross-talk might be mediated by an intravascular MMP-1/PAR1 axis. We postulated that tumor-derived MMP-1 may induce a prothrombotic, proinflammatory, and adhesive milieu via activation of endothelial cells expressing functional PAR1. Accordingly, prothrombotic and proinflammatory conditions were shown to increase tumor progression (16–18). We

Requests for reprints: Stefan W. Schneider, Department of Dermatology, University of Muenster, Von-Esmarch Strasse 58, 48149 Muenster, Germany. Phone: 49-251-83-56525; Fax: 49-251-83-56541; E-mail: sschnei@mednet.uni-muenster.de.

doi:10.1158/0008-5472.CAN-05-3897

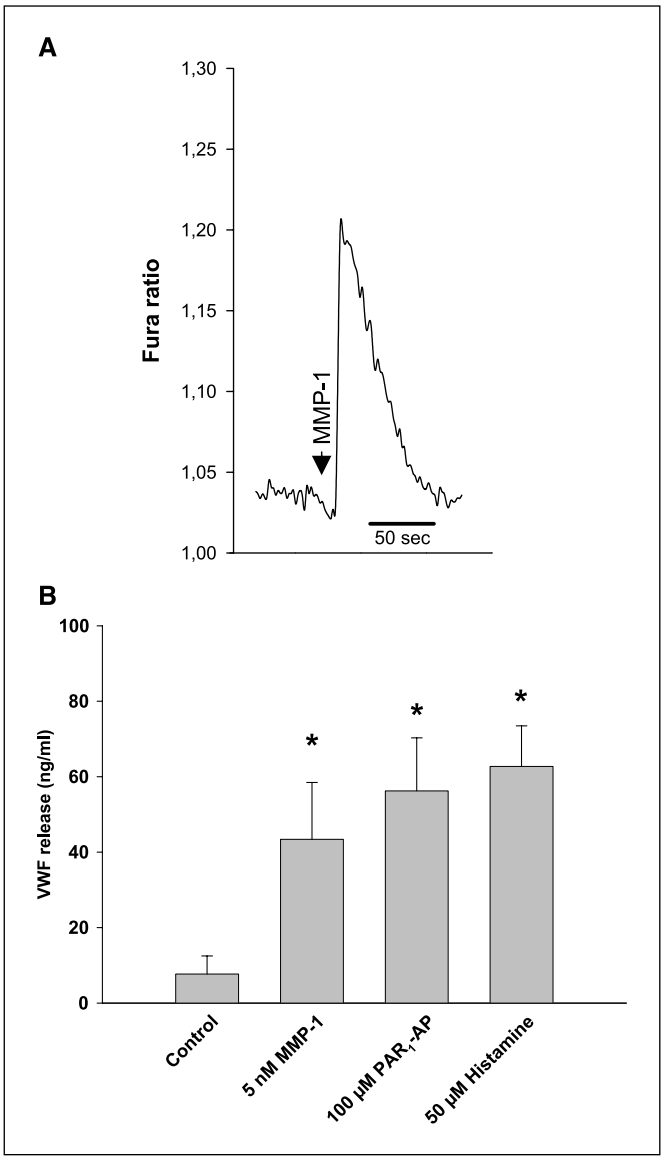

Figure 1. MMP-1 generates Ca^{2+} signals and acute ECA in HUVECs. *A,* calcium flux measurement of HUVECs following challenge with activated MMP-1. Representative tracing of intracellular calcium level increasing from resting 1.02 to 1.2 Fura2 ratio. Experiments were done with emission recorded at 510 nm with dual excitation at 340 and 380 nm. This increase is comparable with the calcium response triggered by PAR1-AP (cf. Fig. 2*B*). *B,* VWF release of stimulated HUVECs. For comparison, HUVECs were stimulated with MMP-1 (5 nmol/L; 43 ± 15 ng/mL), PAR1-AP (100 μmol/L; 56 ± 14 ng/mL), or histamine (50 μmol/L; 62 ± 11 ng/mL; $n = 4$ each).

here show that MMP-1 induces acute endothelial cell activation (ECA) by activation of microvascular and macrovascular endothelial PAR1. Similarly, culture supernatant from tumor cells containing MMP-1 leads to ECA. Inhibition of tumor-derived MMP-1 significantly attenuates tumor-induced ECA and indicates an intravascular MMP-1/PAR1 axis.

Materials and Methods

Reagents, antibodies, and buffers. The following reagents were obtained from the indicated providers: blocking PAR1 anti-human PAR1 antibody ATAP-2 and polyclonal anti-human PAR1 antibody H111 (Santa Cruz Biotechnology, Heidelberg, Germany), pro-MMP-1 and MMP inhibitor I (FN-439; Calbiochem, Bad Soden, Germany), anti-human von Willebrand factor (VWF; DAKO, Hamburg, Germany), anti-human MMP-1 antibody (Chemicon, Hofheim, Germany), PAR1-AP and SCH-79797 (Bachem, Weil am Rhein, Germany), and hirudin (Pentapharm, Munich, Germany). RWJ-58259 was kindly provided by J&J Pharmaceuticals (Springhouse, NJ). Cells were incubated in HEPES-buffered Ringer solution (HBRS) consisting of 140 mmol/L NaCl, 5 mmol/L KCl, 1 mmol/L $MgCl_2$, 1 mmol/L $CaCl_2$, 5 mmol/L glucose, and 10 mmol/L HEPES. Activation of pro-MMP-1 was done according to provider's instructions using p-aminophenylmercuric acetate (APMA). Alternatively, pro-MMP-1 was added to HBRS on thawing in final concentration of 5 nmol/L and incubated in a 37°C water bath. Autocatalytic activation occurred in a time-dependent manner with stable activity after 4 hours. Preliminary studies showed that autocatalytic activated MMP-1 was equally effective as APMA-activated MMP-1 in endothelial PAR1 stimulation.

Cell culture. Human umbilical vein endothelial cells (HUVEC) and human dermal microvascular endothelial cells (HDMEC) were isolated and grown in culture as described (19, 20). For experiments, we used confluent endothelial cells <10 days (passage 1). The culture medium (Life Technologies, Karlsruhe, Germany) contained 10% heat-inactivated FCS (Boehringer Mannheim, Mannheim, Germany), antibiotics (penicillin and streptomycin), 5 units/mL heparin (Biochrom, Berlin, Germany), and 1 mL/100 mL growth supplement derived from bovine retina as described (21). Human melanoma cell lines (A7, WM9, and A375) and colon cancer cell lines (HT-29 and Caco-2) were incubated in a standard culture medium containing enriched Earle's salts, nonessential amino acids, glutamic acid, and 10% FCS (Biochrom; ref. 15).

Production of tumor-derived supernatant. For a standardized generation of tumor culture supernatant, human tumor cells were cultured in a T75 flask. When grown to confluence, standard culture medium was removed, and cells were rinsed intensely thrice in 15 mL HBRS to wash out culture medium remains. After incubation for 6 hours in 5 mL HBRS, conditioned tumor-derived supernatant was harvested from the intact cell layer and centrifuged to downspin membrane debris, and the upper portion was frozen away as tumor derived supernatant for experiments.

Fluorescence-activated cell sorting. Briefly, HUVECs (0.5×10^6) and HDMECs (0.5×10^6) were used for PAR1 surface expression analysis. Cells were fixed with 2.5% paraformaldehyde for 15 minutes on ice, washed twice in PBS (1% FCS), and subsequently incubated with primary rabbit anti-human PAR1 polyclonal antibody (1 μg/mL) for 30 minutes on ice. To detect anti-PAR1 primary antibody, cells were additionally washed twice in PBS (1% FCS) after the first incubation on ice and then incubated with FITC-conjugated pig anti-rabbit secondary antibody (1:200 dilution; DAKO) in PBS (1% FCS) for additional 30 minutes on ice. After two more washes with PBS (1% FCS), cells were resuspended in 300 μL PBS (1% FCS) for analysis. Cells that were incubated with FITC-conjugated secondary pig anti-rabbit antibody alone served as a negative control. At least 20,000 of stained cells were analyzed with the FACSCalibur and CellQuest Pro Software (Becton Dickinson, Heidelberg, Germany).

VWF-ELISA. For all experiments, endothelial cells were grown to confluence in commercially available tissue culture 12-well plates. For experiments, culture medium was removed, and cells were incubated after washing thrice in HBRS. For stimulation, activators and inhibitors were added to HBRS at indicated concentrations. The supernatant of endothelial cells of experimental and control groups were harvested after 15 minutes, cleared of cell debris by centrifugation, and immediately stored at −20°C for later VWF analysis. The release of VWF was measured by a sandwich ELISA technique using a polyclonal rabbit anti-human VWF antibody and a polyclonal rabbit peroxidase-labeled anti-human VWF antibody. The standard curve was generated using purified VWF protein (Calbiochem). Due to the known constitutive release of VWF and heterogeneity of endothelial cells for some experiments, values are given in relation to basal secretion, which is set to 100%.

Measurements of intracellular calcium. Measurements of intracellular calcium were done as described previously (21). In brief, endothelial cells were cultured on glass coverslips coated with 0.5% gelatin. After the cells were grown to confluency, they were loaded with 4.5 μmol/L Fura2 in HBRS

for 10 minutes at room temperature. Then, the coverslips were mounted on a temperature-controlled (37°C) microscope tissue chamber and washed thrice with HBRS before the onset of continuous superfusion. Fields of about eight cells were visualized on a Nikon (Diaphot 300, Nikon, Düsseldorf, Germany) inverted microscope and excited alternately at 340 and 380 nm. The fluorescence emission was measured at 510 nm using a photon counting detector. The tracings (340 and 380 nm) were corrected in each experiment for autofluorescence before calculating the 340:380 ratio.

Western blotting analysis. Proteins in 20 mL tumor-derived supernatant were precipitated in an ice-cooled 10% solution of trichloracetic acid. Precipitates were washed in acetone and solubilized in loading buffer. Equal volume samples were separated by denaturizing SDS-PAGE and electrotransferred to nitrocellulose membranes as described previously (15). After incubation with MAB 13402, a monoclonal mouse anti-human MMP-1 antibody and peroxidase-conjugated secondary antibodies, blots were developed with SuperSignal chemiluminescent substrate (Pierce Biotechnology, Bonn, Germany). The antibody was also applied for immunofluorescence staining.

Interleukin-8 ELISA. Cell supernatants were assayed for interleukin-8 (IL-8) by ELISA. Briefly, polystyrene 96-well plates were coated with polyclonal goat anti-human IL-8 antibody (R&D Systems, Wiesbaden, Germany) diluted in PBS as capture antibody. Polyclonal rabbit anti-human IL-8 (Endogen, Bonn, Germany) was used as detection antibody followed by incubation with a horseradish peroxidase (HRP)–labeled donkey anti-rabbit IgG. Bound HRP was visualized with tetramethylbenzidine (Sigma, Munich, Germany) and H_2O_2 diluted in sodium acetate buffer (pH 6.0). The color reaction was stopped by addition of 1.2 mol/L H_2SO_4, and absorbance was measured at 450 nm. IL-8 concentrations were calculated from standard curves using recombinant human IL-8 (R&D Systems). Endogenous IL-8 from tumor-derived supernatants was subtracted.

Collagenase activity assay. Supernatants from melanoma and colon cancer cells were assessed for their ability to cleave biotinylated collagen in a commercially available collagenase activity assay (Chemicon). The standard curve was generated with pure MMP-1, thus ensuring a quantification of enzyme activity.

Statistical analysis. Mean data of experiments are given ±SE. Statistical significance was tested with unpaired Student's t test. $P \leq 0.05$ indicates a significant difference to control values.

Results

MMP-1 induces mobilization of intracellular Ca^{2+} and VWF release in human primary endothelial cells. It was shown recently that tumor-expressed PAR1 is proteolytically cleaved by MMP-1 (12). To reveal whether active MMP-1 induces functional responses in endothelium, which is known to express PAR1, we examined changes of $[Ca^{2+}]_i$ and VWF release by endothelial cells on enzyme stimulation.

In the first series of experiments, we measured intracellular calcium concentrations in HUVECs on stimulation with activated MMP-1 using fluorescence spectrophotoscopy as published previously (21, 22). Figure 1*A* displays the representative tracing of quiescent endothelium challenged with active MMP-1 (5 nmol/L). HUVECs respond to MMP-1 with an immediate calcium increase as measured by Fura2 ratio (δ Fura ratio, 0.17 ± 0.031; n = 5).

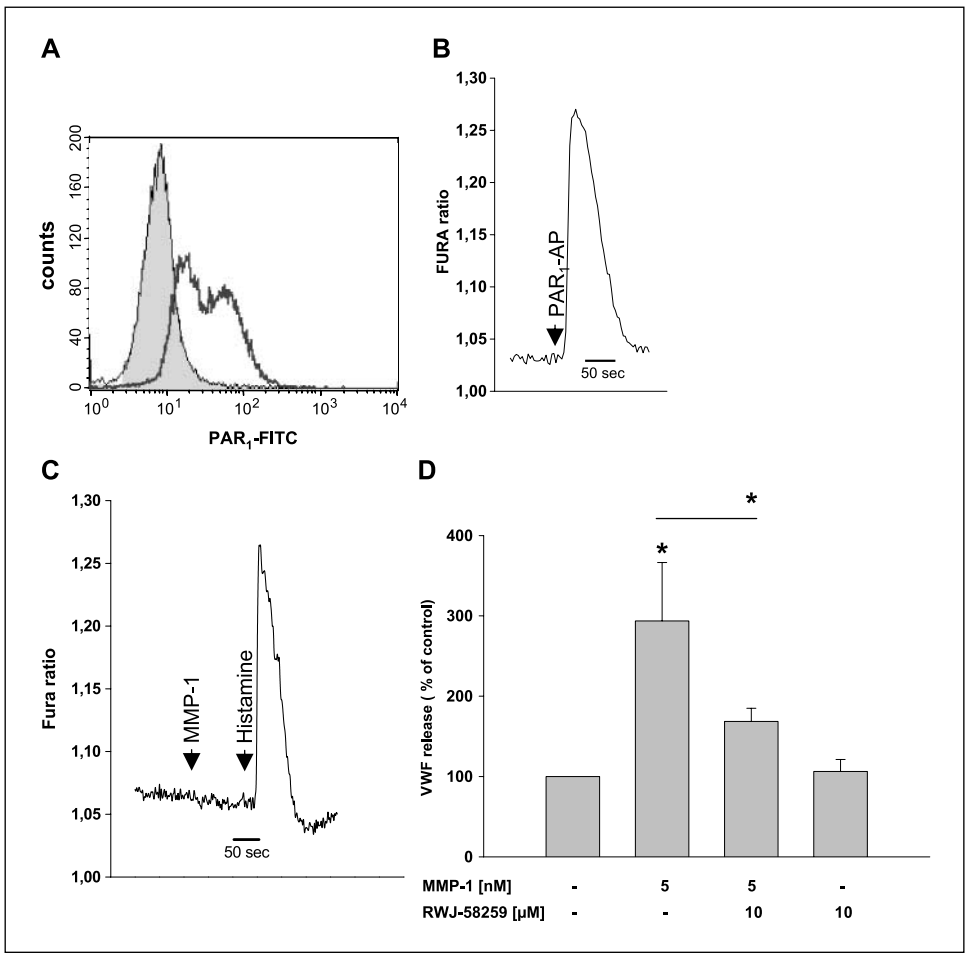

Figure 2. Inhibition of MMP-1-induced ECA by PAR antagonists. *A,* HUVECs at passage 1 were analyzed for expression of PAR1. PAR1 is expressed in ~70% of analyzed cells in flow cytometry. *Gray-shaded peak,* control Ig antibody; *dark gray line,* anti-PAR1 antibody. *B,* representative tracing of calcium flux measurement of HUVECs following challenge with a specific PAR1-activating peptide. PAR1-AP induces an instant sharp Ca^{2+} peak with an increase of Fura2 ratio from 1.03 to 1.27. *C,* calcium flux measurement in HUVECs pretreated with the PAR1 antagonist SCH-79797 (1 μmol/L). Challenge with activated MMP-1 does not elicit an increase of intracellular calcium concentration (n = 5) as seen before (cf. Fig. 1*A*). However, subsequent stimulation with histamine (50 μmol/L) still elicits a calcium flux, showing endothelial integrity. *D,* inhibition of MMP-1-induced VWF release by blockage of endothelial PAR1. Release of VWF is displayed in relation to unstimulated control considering the constitutive basal VWF secretion of endothelial cells (n = 4 for each). Application of PAR1 inhibitor RWJ-58259 significantly blocks endothelial activation (from 293 ± 73% to 168 ± 16%). Inhibitor alone does not affect VWF release.

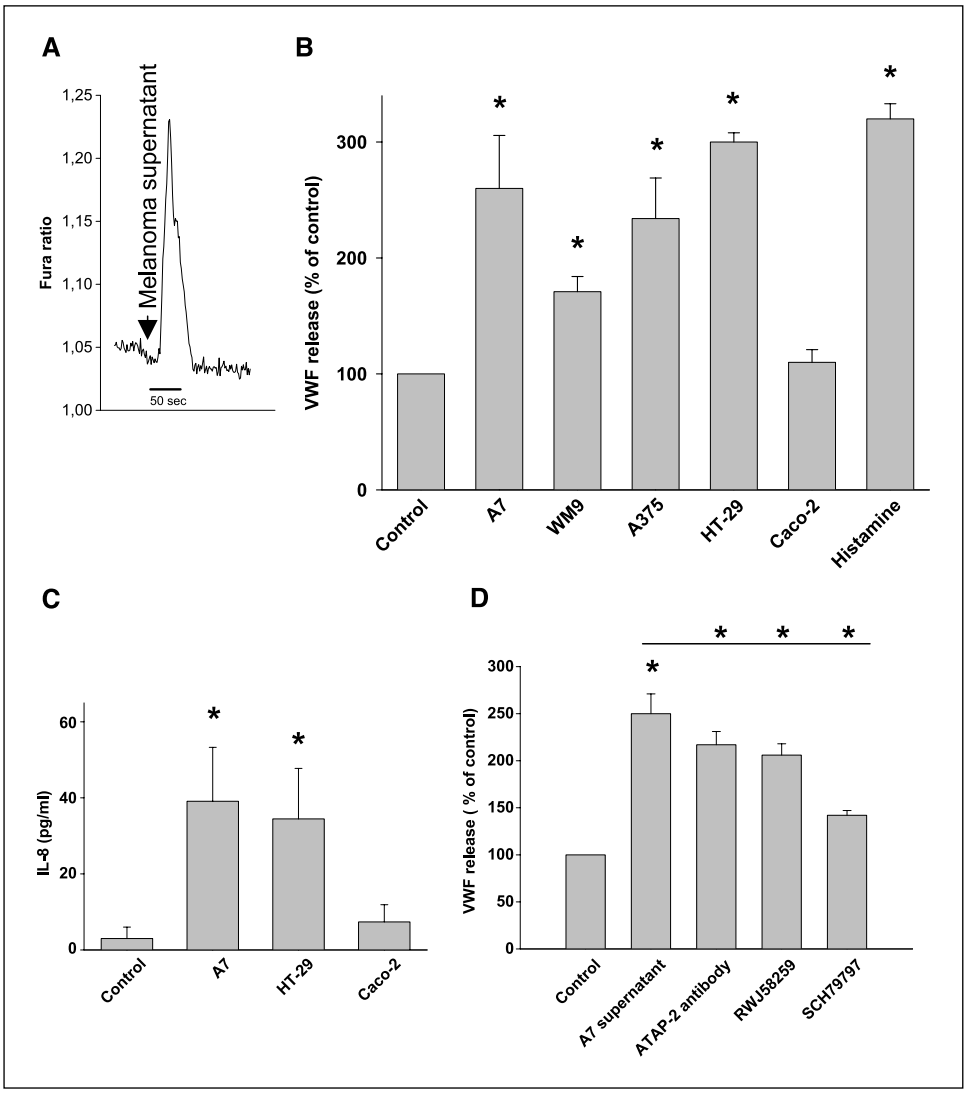

Figure 3. Tumor-derived supernatant induces acute endothelial activation that can be inhibited by PAR1 antagonism. *A,* calcium flux in HUVECs following challenge with A7 melanoma cell–derived supernatant. Stimulation with A7 supernatant rapidly induces a sharp increase of intracellular calcium with an invariable increase of Fura2 ratio from 1.04 to 1.23 resembling results from MMP-1 stimulation. *B,* supernatant-induced endothelial activation assessed by VWF-ELISA. Summarized results from individual experiments are given with constitutive VWF secretion of HUVEC set to 100%. Supernatant from low metastatic Caco-2 cells fails to elicit a significant VWF release in contrast to high metastatic A7, A375, WM9, and HT-29 tumor cells. Histamine-induced release is given as a reference. *C,* measurements of IL-8 release from stimulated HUVEC. Significant amounts of IL-8 were released in response to A7 and HT-29 but not Caco-2 supernatant (39 $\pm$ 10, 34 $\pm$ 9, and 7 $\pm$ 4 pg/mL; n = 4 each). *D,* blockage of endothelial PAR1 significantly attenuates VWF exocytosis. For PAR1 inhibition, a blocking monoclonal antibody (20 μg/mL ATAP2) and peptide-mimetic inhibitors (RWJ-58259 and SCH-79797) were used. SCH-79797 blocks VWF release from 250 $\pm$ 21% to 142 $\pm$ 5% of stimulated VWF release.

We observed that MMP-1-induced calcium peaks in HUVECs desensitize the cells, as repeated stimulation failed to elicit further calcium peaks (data not shown). This observation points to a signaling mechanism mediated by a functional receptor. Of note, only activated MMP-1 induced a detectable intracellular calcium peak, further underlying a specific interaction of the proteolytically active MMP and its substrate. MMP-1, a novel activator of PAR1, induced an intracellular calcium increase, which resembles PAR1-AP-induced calcium values (cf. Fig. 2*B*).

To further analyze the functional role of MMP-1-induced calcium signaling in endothelial cells, we measured exocytosis of VWF, a marker for acute ECA (see Discussion). The glycoprotein VWF is stored in intracellular secretory granules called Weibel-Palade bodies (WPB). These vesicles also contain P-selectin, a crucial promoter of inflammation and thrombosis (23). Regulated exocytosis of VWF is inducible by several secretagogues acting, among others, via the thrombin receptor PAR1 (24). As detected by VWF-ELISA (Fig. 1*B*), MMP-1 (5 nmol/L) stimulated a regulated release of VWF from endothelial cells. The constitutive release of VWF (25) accounts for the results in the control group. For comparison, the extent of VWF exocytosis by the known secretagogues PAR1-AP (100 μmol/L) and histamine (50 μmol/L) is indicated. This experiment shows for the first time that, indeed, MMP-1 is a potent agonist inducing the activation of endothelial cells.

Inhibition of MMP-1-induced ECA by PAR1 antagonists. We next examined whether MMP-1-induced activation of HUVECs is mediated by endothelial PAR1. HUVECs were used at passage 1 throughout all experiments (see Materials and Methods) and found in fluorescence-activated cell sorting (FACS) analyses to express high levels of PAR1 (Fig. 2*A*). Functional activity of endothelial PAR1 was proven by measurement of intracellular calcium flux. To avoid costimulation of other PARs, as reported for thrombin (26), we used a specific (TFLLR-NH2) PAR1-activating peptide (δ Fura ratio, 0.24 $\pm$ 0.009; n = 4, Fig. 2*B*; ref. 3).

To further validate that MMP-1-induced ECA is specifically mediated via endothelial PAR1, we antagonized cellular calcium response using specific PAR1 antagonists (2). As shown in Fig. 2*C*, the MMP-1-induced increase of intracellular calcium was antagonized by SCH-79797 (1 μmol/L), a peptide-mimetic antagonist of PAR1 (27). RWJ-58259 (10 μmol/L), another PAR1 antagonist (28), had a similar inhibitory effect (data not shown). To exclude a reduced MMP-1-elicited calcium peak due to putative depletion of

intracellular calcium stores, endothelial cells were postexperimentally stimulated with histamine (50 μmol/L), a PAR1-independent agonist (29). Activation of histamine receptors promptly elicited a calcium flux, showing endothelial cell integrity (Fig. 2*C*).

As it is known that PAR1 activation orchestrates a variety of endothelial responses, we examined whether PAR1 antagonism would inhibit the effect of MMP-1-induced ECA. Therefore, we investigated WPB exocytosis via VWF-ELISA. HUVECs were pretreated with a PAR1 antagonist before stimulation with MMP-1. As shown in Fig. 2*D*, MMP-1-induced VWF exocytosis was significantly inhibited by RWJ-58259 (from 293 ± 73% to 168 ± 16%; $n = 4$ each). The control release due to constitutive secretion of VWF by HUVEC was set to 100%. The fact that MMP-1-induced ECA was not completely inhibited by the PAR1 antagonist might be attributable to incomplete PAR1 inhibition and/or endothelial costimulation independent of PAR1 assigned to WPB exocytosis independent of calcium signaling. However, VWF release was significantly reduced after PAR1 antagonism. These findings show that MMP-1 exerts its effects on human endothelial cells, at least in part, via PAR1.

Tumor-derived soluble factors activate endothelial cells through PAR1. Our previous results show that the concept of MMP-1/PAR1 communication proves efficient in a setup where purified MMP-1 activates PAR1 on endothelial cells. In further experiments, we analyzed whether tumor-derived soluble factors elicit a calcium response and promote ECA.

Challenging a quiescent HUVEC monolayer with culture supernatant from A7 melanoma cells resulted in an immediate increase of the intracellular calcium concentration (δ Fura ratio, 0.21 ± 0.011; $n = 9$). As indicated by a representative tracing in Fig. 3*A*, HUVECs responded to melanoma-derived supernatant with an immediate calcium flux, resembling the previously

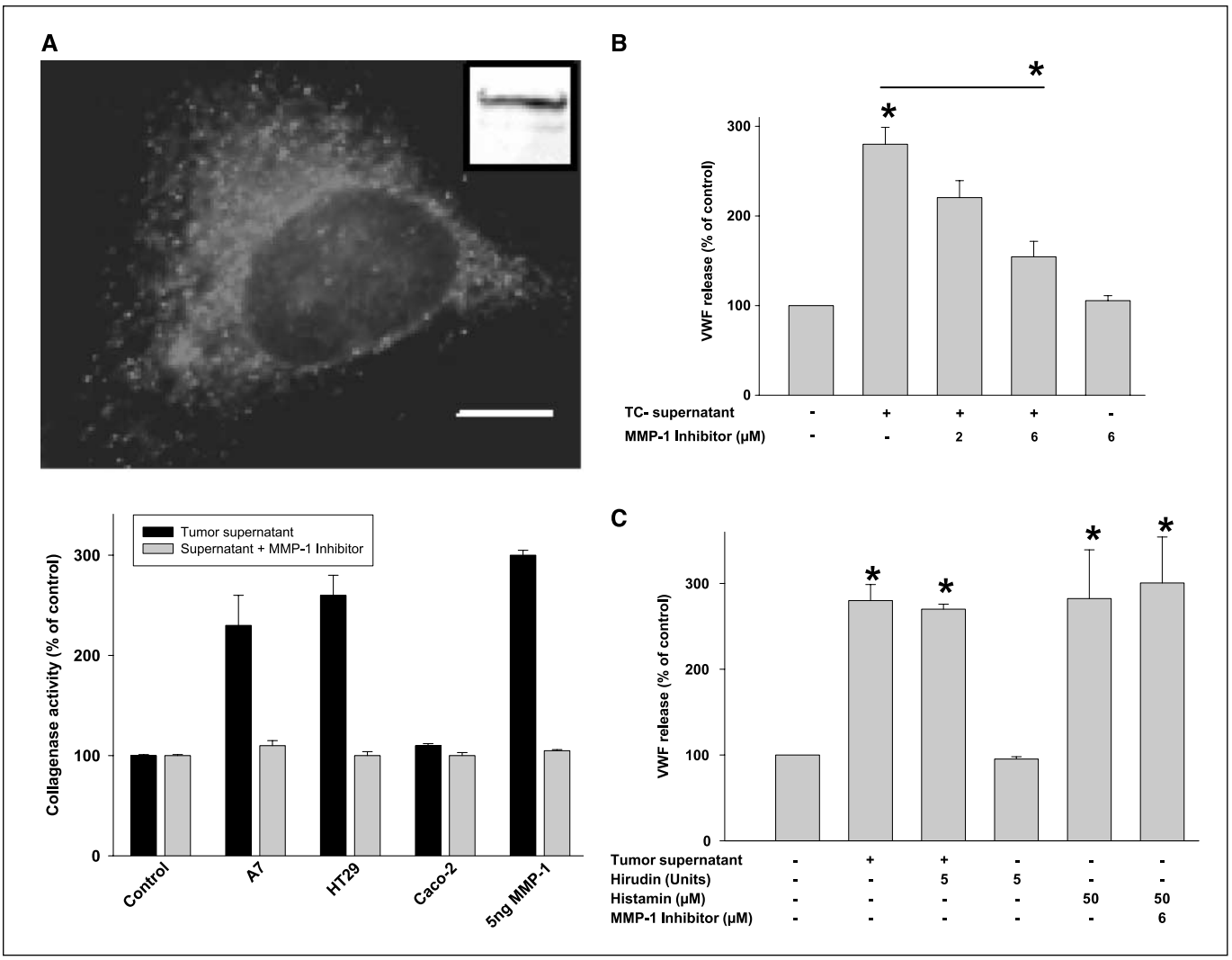

Figure 4. Heterogeneity of tumor-derived MMP-1 secretion and inhibition of ECA. *A,* immunofluorescence staining of A7 melanoma cells reveals the vesicular distribution of intracellular MMP-1. Bar, 5 μm. *Inset,* Western blot analysis of culture supernatant detects soluble MMP-1. MMP-1 activity was assessed in a collagenase activity assay. A7 and HT-29 supernatants display high enzyme activitiy, which is almost undetectable in Caco-2. MMP-1 inhibitor FN-439 proves efficient for MMP-1 inhibition. *B,* ECA induced by melanoma and colon cancer supernatant is inhibited by a highly effective inhibitor of MMP-1 (FN-439). FN-439 attenuates VWF release in a concentration of 2 μmol/L and significantly blocks ECA at 6 μmol/L (from 280 ± 19% to 154 ± 17%). The inhibitor has a relevant IC_{50} for MMP-1 of 1 μmol/L and does not effect basal VWF secretion ($n = 6$ each). *C,* control experiments that rule out a possible role for tumor-generated thrombin in our setup. Hirudin (5 units) did not significantly diminish VWF exocytosis ($n = 6$). FN-439 was shown not to inhibit stimulated VWF release unspecifically, as histamine-induced VWF release was unaffected.

obtained results from PAR1-AP and activated MMP-1 (cf. Figs. 1*A* and 2*B*). The response was invariably reproduced with supernatants from different melanoma cell lines (A375 and WM9; data not shown). Our results show clearly that soluble factors secreted by melanoma cells are capable of stimulating endothelial cells in a paracrine manner.

Subsequently, we examined whether culture supernatant from melanoma and colon cancer cells causes VWF release from WPBs. Tumor cell–derived supernatant (A7, A375, WM9, and HT-29) induced ECA, as displayed by a significant increase of secreted VWF protein (Fig. 3*B*). To compare the extent of endothelial activation, histamine-induced VWF release was given as a reference. Endothelial activation by supernatant from metastatic tumors was almost equivalent to histamine (50 μmol/L), one of the most potent activators of vascular endothelium. It is interesting to observe that there is virtually no ECA by the low metastatic cell line Caco-2 (110 ± 11% of baseline; $n = 5$).

We further assessed whether culture supernatant would induce endothelial IL-8 secretion as an additional variable for PAR1 activation. As shown in Fig. 3*C*, endothelial cells respond to stimulation with culture supernatant with an immediate release of IL-8 that was found to be statistically significant in the metastatic tumor cell lines.

Due to the fact that tumor cells are known to produce an armada of secretory proteins acting on endothelial receptors, we examined the role of endothelial PAR1 as a putative receiver in tumor-host communication. As presented, inhibition of endothelial PAR1 by different PAR1 inhibitors (SCH-79797, RWJ-58259, and ATAP-2) significantly decreased VWF release and thus ECA (from 251 ± 21% to 142 ± 5%; $n = 6$ each; Fig. 3*D*). Incomplete inhibition of ECA may be noticed because of other tumor-derived proteins, which are capable of inducing VWF release independent of PAR1. What is more, the need for more effective means of PAR1 inhibition has been discussed recently (30). However, the major fraction of VWF release was clearly associated with PAR1 activation.

Inhibition of tumor-secreted MMP-1 attenuates ECA. We have shown that blockage of endothelial PAR1 attenuates tumor supernatant-induced ECA. Next, we wanted to prove that endothelial PAR1 activation was associated specifically with release of tumor-derived MMP-1. Immunofluorescence stainings for MMP-1 and Western blot analysis of melanoma culture supernatant were done as reported previously (15). Here, we show the vesicular distribution of MMP-1 stored intracellulary and released into the culture supernatant (Fig. 4*A, top*). In addition, we assessed culture supernatants in their ability to cleave collagen in a specific collagenase activity assay. As shown in Fig. 4*A* (*bottom*), enzyme activity significantly differs between tumor cell lines. The highest collagenotic activity is found in those supernatants that showed previously the highest endothelial activation (cf. Fig. 3*B*). MMP-1 inhibition efficiently blocks collagenase activity, indicating MMP-1 is the most important protease in this assay.

To prove the functional relevance of tumor-derived MMP-1 on ECA, we did inhibition studies using the well-characterized MMP-1 inhibitor FN-439 (31). As shown in Fig. 4*B*, induction of ECA by melanoma-derived supernatant was significantly attenuated (from 280 ± 19% to 154 ± 17%; $n = 6$ each) by the MMP-1 inhibitor. Similar values were obtained for HT-29 supernatant (data not shown). Inhibition of VWF release was dose dependent with significant suppression at reliable MMP-1 inhibitor concentrations (>3× IC50). FN-439 itself did not influence VWF constitutive release. Specificity of FN-439 was further shown by not affecting histamine-induced VWF release (Fig. 4*C*). To rule out a possible role of tumor-generated thrombin in our setup (32), we did inhibition studies with hirudin. There was no significant inhibition of supernatant-induced ECA as seen with the MMP-1 inhibitor (Fig. 4*C*).

A functional MMP-1/PAR1 axis in primary microvascular endothelial cells. To further show the concept of tumor-endothelial communication, we did another series of experiments with microvascular endothelial cells. These cells are known to play a predominant role in the process of metastasis and angiogenesis. Isolated MMP-1 (5 nmol/L) invariably produced a calcium flux signal (δ Fura ratio, 0.1 ± 0.02; $n = 4$; Fig. 5*A*), and a significant release of VWF could be detected (219 ± 20%; $n = 6$; Fig. 5*B*). FACS analysis proved the presence of PAR1 in cultured HDMECs (Fig. 5*B, inset*). Inhibition studies with PAR1 antagonist SCH-79797 revealed a significant dose-dependent reduction of VWF release (from 196 ± 21% to 139 ± 8%; Fig. 5*C*). Addition of MMP-1 inhibitor FN-439 to culture supernatant significantly blocked stimulated release (from 158 ± 9% to 124 ± 3%; $n = 6$ each), thus indicating a functional MMP-1/PAR1 axis in the microvasculature (Fig. 5*D*).

Our experiments show that culture supernatant from tumor cells strongly affects endothelial cell integrity. This activation was substantially mediated via endothelial PAR1, which was cleaved by tumor-secreted MMP-1. Therefore, our findings reveal a novel tumor-endothelial communication pathway based on a functional intravascular MMP-1/PAR1 axis inducing a signaling cascade leading to ECA (Fig. 6).

Discussion

In the present study, we report for the first time that antagonism of either endothelial PAR1 or tumor-derived MMP-1 significantly decreases tumor-induced activation of vascular endothelial cells. This main finding of our study reveals the existence of a previously undescribed pathway of tumor-endothelial communication that relies on a novel functional intravascular MMP-1/PAR1 axis. A tumor-secreted protease (MMP-1) interacts with a signal-mediating receptor (endothelial PAR1) promoting ECA. This discovery inverts the reported concept of MMP-1/PAR1 interaction, where host-derived MMP-1 activates tumor-expressed PAR1, and transfers this pathway of intercellular communication to a completely new locus of tumor-host interaction: the vascular system.

Several studies clearly indicate an important role of tumor-expressed PAR1 in tumorigenesis of various tissues (4–7). However, little is known about the role of tumor-derived MMP-1 activating endothelial PAR1.

MMPs represent a family of zinc-dependent endopeptidases, which are able to degrade virtually any component of the extracellular matrix (ECM). To date, 24 members of this family have been identified in humans. MMPs are critical for remodeling the ECM, thereby affecting cell behavior under physiologic and pathophysiologic circumstances, such as embryogenesis and cancer progression (33). Available data suggest that activation of different MMPs during cancer progression is a phase-dependent process, making the recognition of individual MMPs and their early roles for invasion indispensable (34). In the present study, challenging vascular endothelium with activated MMP-1 resulted in an immediate ECA displayed by calcium flux and WPB exocytosis (Figs. 1, 2, and 5). We showed that a MMP specifically interacts with vascular endothelium causing ECA. Using specific peptide-mimetic antagonists (SCH-79797 and RWJ-58259), we are

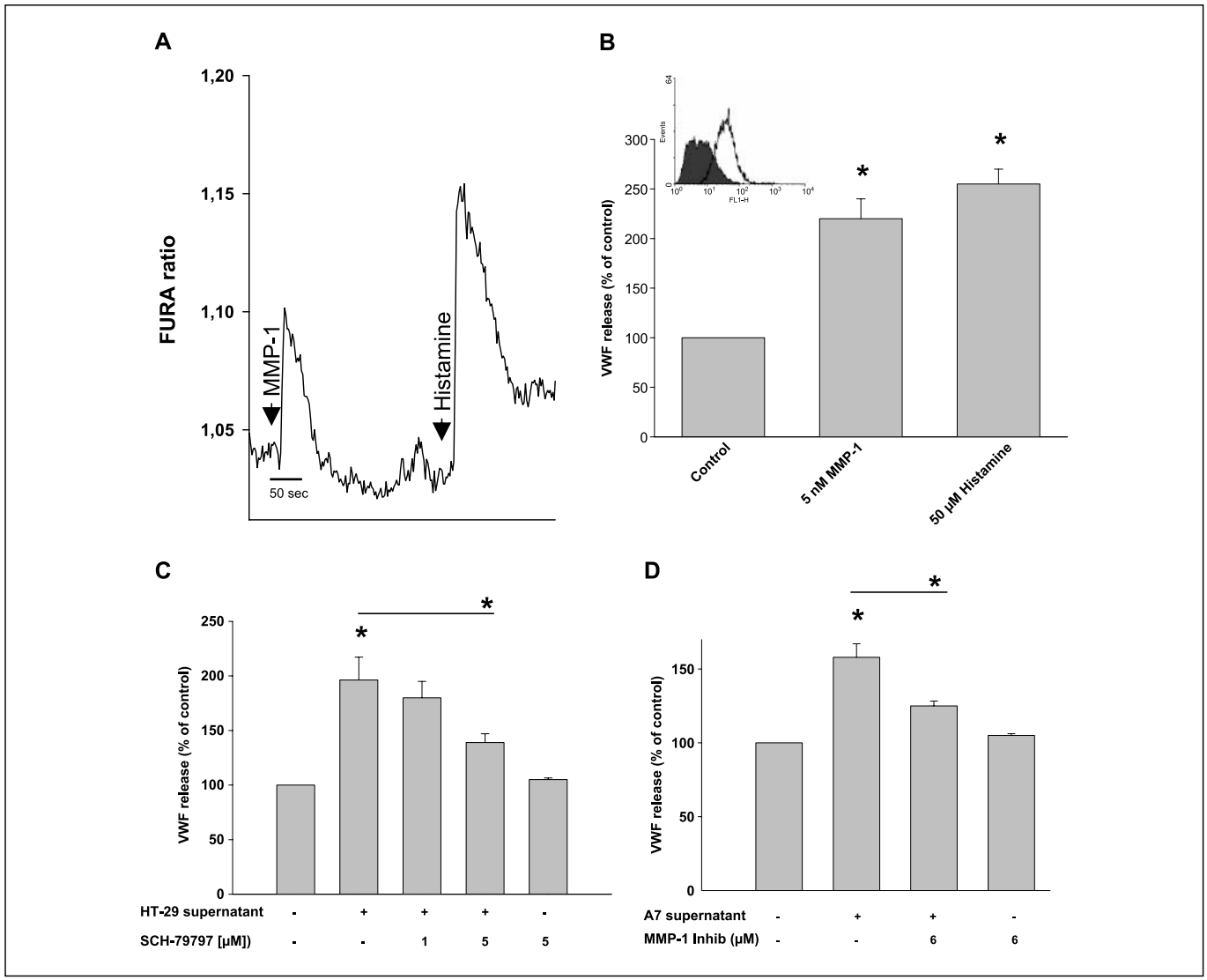

Figure 5. Analysis of a functional MMP-1/PAR1 axis in primary microvascular endothelium. *A,* calcium flux measurement of HDMEC following challenge with activated MMP-1. Representative tracing of intracellular calcium level increasing from resting 1.03 to 1.1 Fura2 ratio. For comparison, endothelium was challenged with histamine (50 μmol/L). Although overall reactivity of HDMEC was found to be inferior compared with HUVEC, the ratio of stimulated and basal VWF secretion was found to be similar. *B,* VWF release of MMP-1-stimulated HDMEC. VWF-ELISA results are shown in percentage of control. HDMECs were stimulated with MMP-1 (5 nmol/L) and histamine (50 μmol/L). *Inset,* PAR1 is expressed in ~75% of analyzed cells in flow cytometry. *Gray-shaded peak,* control Ig antibody; *dark gray line,* anti-PAR1 antibody. *C,* antagonism of PAR1 significantly reduces tumor cell supernatant-induced VWF release in HDMEC. *D,* supernatant-induced ECA is significantly inhibited by MMP-1 inhibitor FN-439. The inhibitor does not affect basal VWF secretion.

able to show that this activation is mediated by endothelial PAR1. These results are in line with the recent observation of Boire et al. (12) who elegantly showed that PAR1 is directly activated by the interstitial collagenase MMP-1. In the same study, it was further revealed that tumor-expressed PAR1 cleavage by stromal (fibroblast derived) MMP-1 plays an important role in the promotion of breast cancer cell invasion. Based on these observations, MMP-1/PAR1 interaction shows that host-derived MMP-1 activates tumor-expressed PAR1 (13). This concept relies on the fact that tumor cells express PAR1, whereas MMP-1 is undetectable in MDA-MB-231 breast cancer cells (12). Here, we report melanoma and colon cancer cell lines that express MMP-1.

Indeed, there are controversial reports about the ability of tumor cells to secrete MMP-1. It was shown previously for different melanoma cell lines that the overexpression of MMP-1 promotes an invasive phenotype (35). Additionally, recent reports proposed a prognostic potential of MMP-1 secretion for patients suffering from breast cancer and malignant melanoma (36, 37). Our group reported previously a highly invasive melanoma cell line (A7) constitutively secreting MMP-1 (14). Our discovery of MMP-1-induced ECA and the ability of melanoma cells to release MMP-1 led us to hypothesize that tumor cells may communicate with host-expressed PAR1 via an intravascular MMP-1/PAR1 axis.

Stimulation of endothelial cells with culture supernatant from melanoma cells immediately induces massive ECA assessed by calcium flux measurements (Fig. 3*A*). Tumor cell–induced calcium fluxes in endothelial cells have been reported previously for murine melanoma and prostate cancer cells. However, in these studies, the physical contact of tumor and endothelium was necessary for the intracellular calcium signaling pathway (38). In our setup, challenging of endothelial cells with melanoma cell–derived supernatant invariably induced an intracellular calcium flux. This

incongruency might be attributable to inconsistent expression of MMP-1 among tumor cell lines (cf. Fig. 4*A*).

Assessing the functional role of supernatant-derived calcium increase, we detected an acute exocytosis of WPBs, indicating promotion of thrombotic and inflammatory cell adhesion by tumor-endothelial cross-talk. Tumor cells are known to secrete an array of cytokines and chemokines interacting with endothelium. However, interactions between these two cell types during tumorigenesis are not fully understood (39). Using previously described PAR1 antagonists devoid of PAR1 agonist and thrombin-inhibitory activity (27, 28, 40), we observed that melanoma and colon cancer supernatant-derived ECA is, at least partially, mediated by PAR1 (Figs. 3*D* and 5*C*).

We have documented that blockage of endothelial PAR1 inhibits tumor supernatant-induced ECA. However, it was not yet shown that PAR1 activation is specifically induced by tumor secreted MMP-1. In previous studies, for instance, it was reported that tumor cells are able to generate thrombin (32), the prototypical activator of PAR1, promoting invasion (7). In our experiments, melanoma and colon cancer cells were incubated in HBRS for the preparation of tumor-derived supernatant. Stimulation of HUVEC was also done in HBRS depriving the system of any serum, which might eventually facilitate thrombin generation causing PAR1 activation. In addition, hirudin experiments did not substantially decrease supernatant-stimulated ECA (Fig. 4*C*) in our setting. Thus, as yet identified activators of endothelial PAR1, such as tumor-generated thrombin, could be excluded to account in the present setting for ECA via PAR1. Furthermore, specificity of tumor-derived ECA was shown using the tetrapeptidyl hydroxamic acid, MMP inhibitor FN-439, that targets MMP-1, MMP-8, MMP-3, and MMP-9 (31). This inhibitor dose dependently attenuated ECA induced by tumor-derived supernatant. Although it could be speculated that inhibition of PAR1 activation is not specific for MMP-1, it was shown previously that MMP-8, MMP-3, and MMP-9 do not activate PAR1 (12).

Adopting Laswell's formula of communication (41) to the biological context of tumor-vascular cross-talk, we observe that melanoma cells represent a "sender" that interacts with the "receiver" (endothelial PAR1) using MMP-1 as a "channel" (carrier of information) to transmit the message (Fig. 6): stimulation of endothelial cells and thus generating a prothrombotic, proinflammatory, and cell-adhesive milieu. ECA is believed to promote tumor progression and metastases (11, 17, 18, 42). In the present report, we used the calcium flux, WPB exocytosis, and IL-8 release as surrogate markers of ECA. WPBs contain VWF, P-selectin, and IL-8 (43), strong promoters of thrombosis and inflammation (23). Agonist-induced WPB exocytosis is a well-characterized process with unparalleled kinetics: the activated endothelium generates a prothrombotic/cell-adhesive (VWF) and proinflammatory (P-selectin/IL-8) milieu within seconds, crucial for the adhesion of circulating platelets and immune and tumor cells. This phenotype has been shown to facilitate tumor cell adhesion and invasion (16, 44), whereas IL-8 induces tumor angiogenesis (45). Moreover, the acute kinetics of VWF release rebuts a substantial role for HUVEC-derived MMP-1 stimulating endothelial PAR1 in an autocrine manner. Stroma-derived MMPs are known to activate tumor cells. However, here, we provide additional evidence for an inverse MMP-1/PAR1 communication pathway.

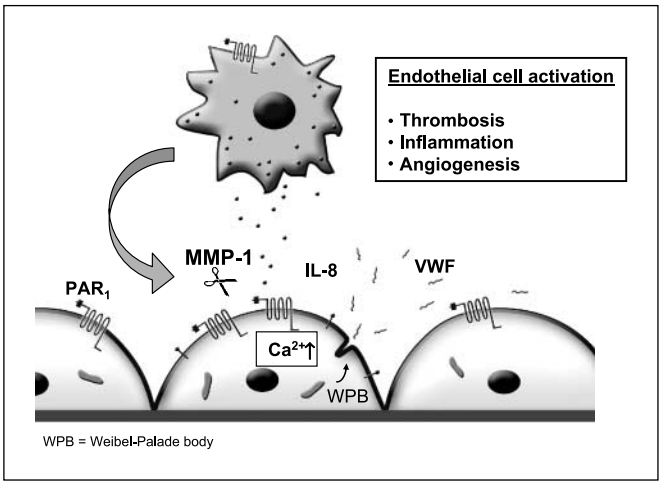

Figure 6. Model of tumor-endothelial communication. Tumor cells (sender) actively secrete MMP-1 (channel) that activates endothelial cells (receiver) via cleavage of PAR1. Our data provide evidence that circulating melanoma cells communicate with endothelium via secreted soluble MMP-1. Interaction of MMP-1 with endothelial cells induces calcium signaling via PAR1 and promotes WPB exocytosis, the endothelial store of prothrombotic, proinflammatory, and proadhesive proteins (VWF, P-selectin, and IL-8). Our findings of metastatic tumor-induced ECA document an intravascular MMP-1/PAR1 axis.

Previously, hematogenous metastasis was shown to be independent of PAR1 in knockout mice (17), a finding that might challenge the relevance of endothelial PAR1 activation by tumor cells. However, our data show the importance of MMP-1 for ECA, and it has to be kept in mind that MMP-1 expression substantially differs between mice and men (46). Mouse melanoma cells used in the above-mentioned study are known to express MMP-2 and MT1-MMP but not MMP-1 (47). The present study observes heterogeneity of MMP-1 expression in various tumor cell lines of different metastatic potential (Fig. 4*A*). In addition, the MMP-1/PAR1 axis was initially discovered in breast cancer cells devoid of MMP-1 activity (12), further underlying heterogeneity of MMP-1 expression. Therefore, different models will have to assess *in vivo* the consequences of MMP-1-induced endothelial PAR1 activation.

In conclusion, we present a novel concept of tumor-endothelial communication based on an intravascular MMP-1/PAR1 axis (Fig. 6). Tumor-derived MMP-1 cleaves microvascular and macrovascular endothelial PAR1, thus generating a prothrombotic and proinflammatory cell surface. Considering the expression pattern of PAR1 on various cell types in the vascular compartment (endothelium, platelets, and neutrophils), it is thrilling to speculate about further tumor-host interactions based on the presented MMP-1/PAR1 axis. It will be the aim of future studies to examine *in vivo* the relative role of the here described MMP-1/PAR1 axis for tumor-induced thrombosis and inflammation.

Acknowledgments

Received 10/31/2005; revised 3/21/2006; accepted 6/2/2006.

Grant support: Young Investigator award from Deutsche Dermatologische Gesellschaft (T. Goerge); Deutsche Forschungsgemeinschaft grants Goe-1360 (T. Goerge), Schn-1071/1-1 (E.M. Schnaeker), SFB 492-A13/B13 (S.W. Schneider and M. Steinhoff), and SFB 293 (M. Steinhoff); Interdisziplinäres Zentrum für Klinische Forschung grant STE2/104/03 (M. Steinhoff); and Innovative Medical Research Münster grant (S.W. Schneider and M. Steinhoff).

The costs of publication of this article were defrayed in part by the payment of page charges. This article must therefore be hereby marked *advertisement* in accordance with 18 U.S.C. Section 1734 solely to indicate this fact.

We thank the gynecologic staff from Raphael Hospital and Franziskus Hospital Münster (Münster, Germany) for providing umbilical cords, Elke Weber for technical assistance, M. Wilhelmi for excellent work in cell culture, Birgit Schneider for the artwork in Figure 6, and Wolfgang Bergmeier and Lesley Cowan for critically reading the article and helpful discussion.

References

1. Coughlin SR. Thrombin signalling and protease-activated receptors. Nature 2000;407:258–64.
2. Ossovskaya VS, Bunnett NW. Protease-activated receptors: contribution to physiology and disease. Physiol Rev 2004;84:579–621.
3. Steinhoff M, Buddenkotte J, Shpacovitch V, et al. Proteinase-activated receptors: transducers of proteinase-mediated signaling in inflammation and immune response. Endocr Rev 2005;26:1–43.
4. Even-Ram S, Uziely B, Cohen P, et al. Thrombin receptor overexpression in malignant and physiological invasion processes. Nat Med 1998;4:909–14.
5. Yin YJ, Salah Z, Grisaru-Granovsky S, et al. Human protease-activated receptor 1 expression in malignant epithelia: a role in invasiveness. Arterioscler Thromb Vasc Biol 2003;23:940–4.
6. Zain J, Huang YQ, Feng X, et al. Concentration-dependent dual effect of thrombin on impaired growth/apoptosis or mitogenesis in tumor cells. Blood 2000;95:3133–8.
7. Nierodzik ML, Chen K, Takeshita K, et al. Protease-activated receptor 1 (PAR-1) is required and rate-limiting for thrombin-enhanced experimental pulmonary metastasis. Blood 1998;92:3694–700.
8. Massi D, Naldini A, Ardinghi C, et al. Expression of protease-activated receptors 1 and 2 in melanocytic nevi and malignant melanoma. Hum Pathol 2005;36:676–85.
9. Nierodzik ML, Plotkin A, Kajumo F, Karpatkin S. Thrombin stimulates tumor platelet adhesion *in vitro* and metastasis *in vivo*. J Clin Invest 1991;87:229–36.
10. Nierodzik ML, Kajumo F, Karpatkin S. Effect of thrombin treatment of tumor cells on adhesion of tumor cells to platelets *in vitro* and tumor metastasis *in vivo*. Cancer Res 1992;52:3267–72.
11. Wojtukiewicz MZ, Tang DG, Ciarelli JJ, et al. Thrombin increases the metastatic potential of tumor cells. Int J Cancer 1993;54:793–806.
12. Boire A, Covic L, Agarwal A, et al. PAR1 is a matrix metalloprotease-1 receptor that promotes invasion and tumorigenesis of breast cancer cells. Cell 2005;120:303–13.
13. Pei D. Matrix metalloproteinases target protease-activated receptors on the tumor cell surface. Cancer Cell 2005;7:207–8.
14. Ludwig T, Ossig R, Graessel S, et al. The electrical resistance breakdown assay determines the role of proteinases in tumor cell invasion. Am J Physiol Renal Physiol 2002;283:F319–27.
15. Schnaeker EM, Ossig R, Ludwig T, et al. Microtubule-dependent matrix metalloproteinase-2/matrix metalloproteinase-9 exocytosis: prerequisite in human melanoma cell invasion. Cancer Res 2004;64:8924–31.
16. Coussens LM, Werb Z. Inflammation and cancer. Nature 2002;420:860–7.
17. Camerer E, Qazi AA, Duong DN, et al. Platelets, protease-activated receptors, and fibrinogen in hematogenous metastasis. Blood 2004;104:397–401.
18. Im JH, Fu W, Wang H, et al. Coagulation facilitates tumor cell spreading in the pulmonary vasculature during early metastatic colony formation. Cancer Res 2004;64:8613–9.
19. Hartmeyer M, Scholzen T, Becher E, et al. Human dermal microvascular endothelial cells express the melanocortin receptor type 1 and produce increased levels of IL-8 upon stimulation with α-melanocyte-stimulating hormone. J Immunol 1997;159:1930–7.
20. Jaffe EA, Nachman RL, Becker CG, Minick CR. Culture of human endothelial cells derived from umbilical veins. Identification by morphologic and immunologic criteria. J Clin Invest 1973;52:2745–56.
21. Goerge T, Niemeyer A, Rogge P, et al. Secretion pores in human endothelial cells during acute hypoxia. J Membr Biol 2002;187:203–11.
22. Steinhoff M, Vergnolle N, Young SH, et al. Agonists of proteinase-activated receptor 2 induce inflammation by a neurogenic mechanism. Nat Med 2000;6:151–8.
23. Wagner DD, New links between inflammation and thrombosis. Arterioscler Thromb Vasc Biol 2005;25:1321–4.
24. Vischer UM, de Moerloose P. von Willebrand factor: from cell biology to the clinical management of von Willebrand's disease. Crit Rev Oncol Hematol 1999;30:93–109.
25. Sporn LA, Marder VJ, Wagner DD. Differing polarity of the constitutive and regulated secretory pathways for von Willebrand factor in endothelial cells. J Cell Biol 1989;108:1283–9.
26. Shi X, Gangadharan B, Brass LF, Ruf W, Mueller BM. Protease-activated receptors (PAR1 and PAR2) contribute to tumor cell motility and metastasis. Mol Cancer Res 2004;2:395–402.
27. Ma L, Perini R, McKnight W, et al. Proteinase-activated receptors 1 and 4 counter-regulate endostatin and VEGF release from human platelets. Proc Natl Acad Sci U S A 2005;102:216–20.
28. Damiano BP, Derian CK, Maryanoff BE, Zhang HC, Gordon PA. RWJ-58259: a selective antagonist of protease activated receptor-1. Cardiovasc Drug Rev 2003;21:313–26.
29. Hamilton KK, Sims PJ. Changes in cytosolic Ca^{2+} associated with von Willebrand factor release in human endothelial cells exposed to histamine. Study of microcarrier cell monolayers using the fluorescent probe indo-1. J Clin Invest 1987;79:600–8.
30. Arribas J. Matrix metalloproteases and tumor invasion. N Engl J Med 2005;352:2020–1.
31. Odake S, Morita Y, Morikawa T, et al. Inhibition of matrix metalloproteinases by peptidyl hydroxamic acids. Biochem Biophys Res Commun 1994;199:1442–6.
32. Fischer EG, Ruf W, Mueller BM. Tissue factor-initiated thrombin generation activates the signaling thrombin receptor on malignant melanoma cells. Cancer Res 1995;55:1629–32.
33. Overall CM, Lopez-Otin C. Strategies for MMP inhibition in cancer: innovations for the post-trial era. Nat Rev Cancer 2002;2:657–72.
34. Coussens LM, Fingleton B, Matrisian LM. Matrix metalloproteinase inhibitors and cancer: trials and tribulations. Science 2002;295:2387–92.
35. Huntington JT, Shields JM, Der CJ, et al. Overexpression of collagenase 1 (MMP-1) is mediated by the ERK pathway in invasive melanoma cells: role of BRAF mutation and fibroblast growth factor signaling. J Biol Chem 2004;279:33168–76.
36. Poola I, DeWitty RL, Marshalleck JJ, et al. Identification of MMP-1 as a putative breast cancer predictive marker by global gene expression analysis. Nat Med 2005;11:481–3.
37. Nikkola J, Vihinen P, Vuoristo MS, et al. High serum levels of matrix metalloproteinase-9 and matrix metalloproteinase-1 are associated with rapid progression in patients with metastatic melanoma. Clin Cancer Res 2005;11:5158–66.
38. Pili R, Corda S, Passaniti A, et al. Endothelial cell Ca^{2+} increases upon tumor cell contact and modulates cell-cell adhesion. J Clin Invest 1993;92:3017–22.
39. Prandoni P, Falanga A, Piccioli A. Cancer and venous thromboembolism. Lancet Oncol 2005;6:401–10.
40. O'Brien PJ, Prevost N, Molino M, et al. Thrombin responses in human endothelial cells. Contributions from receptors other than PAR1 include the transactivation of PAR2 by thrombin-cleaved PAR1. J Biol Chem 2000;275:13502–9.
41. Lasswell H. The structure and function of communication in society. In: Bryson L, editor. The communication of ideas. New York: Harper and Row; 1948.
42. Honn KV, Tang DG, Crissman JD. Platelets and cancer metastasis: a causal relationship? Cancer Metastasis Rev 1992;11:325–51.
43. Romani dW, de Leeuw HP, Rondaij MG, et al. Von Willebrand factor targets IL-8 to Weibel-Palade bodies in an endothelial cell line. Exp Cell Res 2003;286:67–74.
44. Kim YJ, Borsig L, Varki NM, Varki A. P-selectin deficiency attenuates tumor growth and metastasis. Proc Natl Acad Sci U S A 1998;95:9325–30.
45. Sparmann A, Bar-Sagi D. Ras-induced interleukin-8 expression plays a critical role in tumor growth and angiogenesis. Cancer Cell 2004;6:447–58.
46. Newby AC. Dual role of matrix metalloproteinases (matrixins) in intimal thickening and atherosclerotic plaque rupture. Physiol Rev 2005;85:1–31.
47. Hofmann UB, Eggert AA, Blass K, Brocker EB, Becker JC. Expression of matrix metalloproteinases in the microenvironment of spontaneous and experimental melanoma metastases reflects the requirements for tumor formation. Cancer Res 2003;63:8221–5.

Tumor-Derived Matrix Metalloproteinase-1 Targets Endothelial Proteinase-Activated Receptor 1 Promoting Endothelial Cell Activation

Tobias Goerge, Alexej Barg, Eva-Maria Schnaeker, et al.

Cancer Res 2006;66:7766-7774.